African Journal of Biotechnology Vol. 11(18), pp. 4279-4287, 1 March, 2012
Available online at http://www.academicjournals.org/AJB
DOI: 10.5897/AJBX11.040
ISSN 1684–5315 © 2012 Academic Journals

Full Length Research Paper

Theoretical evaluations of electro-manipulation from Jurkat T cells exposed to pulsed electric fields (PEFs) with different time durations

Minghe Wu[1]*, Hongchun Yang[1], Baohua Teng[1], Yu Lei[1], Xiaoming Zheng[2], Mei Zhang[3], Yang Li[1] and Chengli Ruan[1]

[1]School of Physical Electronics, University of Electronics Science and Technology of China (UESTC), 610054, Chengdu, China.
[2]School of Dentistry and Health Science, Charles Sturt University, Wagga Wagga, New South Wales 2678, Australia.
[3]Faculty of Computer, Guangdong University of Technology, Guangzhou 510006, China.

Accepted 3 February, 2012

The multilayer dielectric sphere model (MDSM) was used to analyze responses of Jurkat T cells to pulsed electric fields (PEFs). The dependence of voltages across nuclear plasma, nuclear envelope, cytoplasm and plasma membrane on different time durations of PEFs was calculated by employing the inverse laplace transformation (ILT) in time domain with Maple software. Cytochrome C release was considered as a secondary effect of PEFs when mitochondria substructures were taken into account. It is proposed that two-step process of Cytochrome C release can be realized by bioelectric impulse effect on mitochondria.

Keywords: Laplace transformation, Jurkat T, pulsed electric fields (PEFS), cytochrome C.

INTRODUCTION

The effects of pulsed electric fields (PEFs) on mammalian cells have been explored by some groups (Beebe et al., 2003; Vernier et al., 2004; Weaver and Chizmadzhev, 1996; Kotnik and Miklavcic, 2006; Smith et al., 2004; Hagness et al., 2009). Schoenbach group provided experimental evidence that nanosecond, high intensity pulsed electric fields induce apoptosis and necrosis of Jurkat T cells. This group and other groups gave theoretical explanations on their results in frequency domain on basis of distributed parameter cell model (Schoenbach et al., 2002; Joshi et al., 2004).

In (Yao et al., 2009), for studies on electroporation of plasma membrane and intracellular electro-manipulation (IEM) of cancer cells, electric equivalent model was given where the cytoplasm and nuclear plasma were usually regarded as resistors with neglect of their capacitances while membranes were considered as capacitances without their conductivity. In Kotnik and Miklavcic (2006), both dielectric permittivity and electric conductivity of the organelles were considered but only plasma membrane and organelle membrane are taken into account for explaining why the voltage induced on the organelle membrane can exceed the voltage induced on plasma membrane.

Here, a Jurkat T cell exposed to pulsed electric fields (PEFs) with different time durations is discussed in time domain if the multilayer dielectric sphere model (MDSM) is used for analytic calculation of voltages across the nuclear plasma, nuclear envelope, cytoplasm, plasma membrane. Although, the dielectric permittivity and conductivity of all organelles from Jurkat T are taken into account, it is hypothesized that they are independent of frequencies coming from Fourier analysis for voltages across each of the cell parts. The calculations on basis of Laplace transformation and inverse Laplace transformation will be compared with the reported experimental results from Jurkat T cells (Beebe et al., 2003). If

*Corresponding author. E-mail:wumingheshd@sina.com.

Abbreviations: MDSM, Multilayer dielectric sphere model; **PEFs,** pulsed electric fields; **ILT,** inverse laplace transformation.

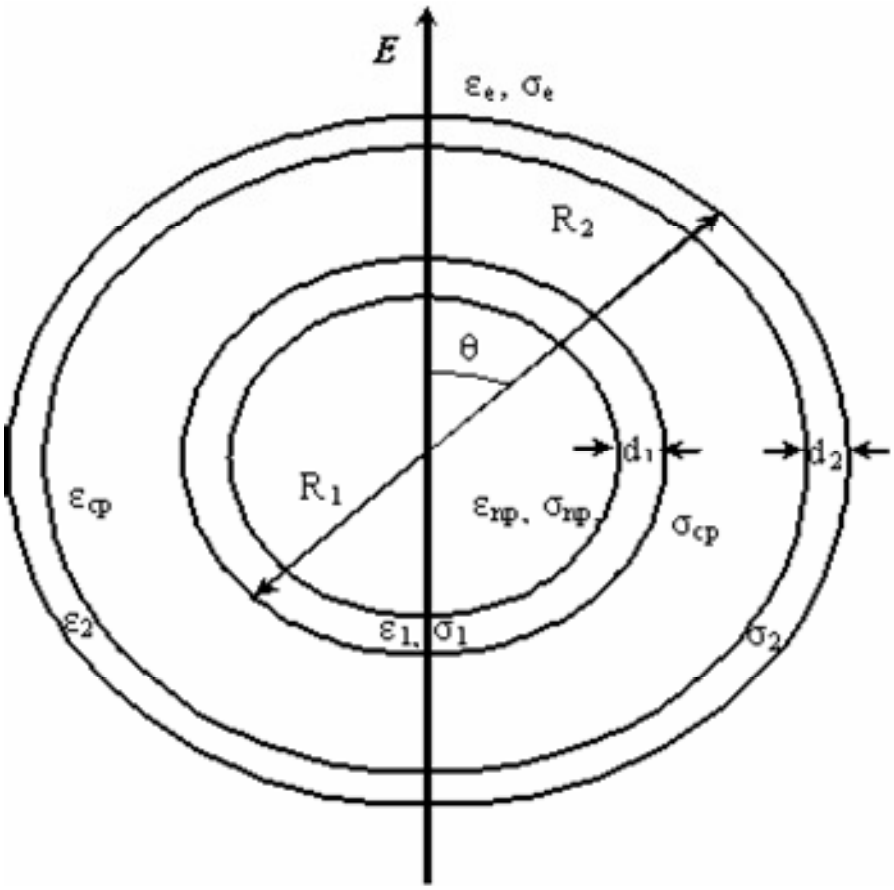

Figure 1. MDSM (Kotnik and Miklavcic 2006) for Jurkat T cells.

apoptosis had been considered as a secondary effect which is closely associated with Cytochrome C release, the voltage across the outer membrane (OM) or voltage-dependent anion channels (VDAC) of mitochondria was calculated with MDSM. Meanwhile impulse effect on positively charged Cytochrome C located in inter-membrane space due to pulsed electric fields on cytoplasm was explained.

METHODOLOGY

MDSM Model

Blood B and T cells have a spherical shape, a thin cell plasma membrane (PM), cytoplasm (CP), nuclear plasma (NP) or nucleus, which occupies 60% of cells volume and have a thin nuclear envelope (NE) (Ermolina et al., 2001). At the beginning of the manuscript, the sub-cell structures of cell in cytoplasm, such as Golgi apparatus, endoplasmic reticulum (ER) and mitochondria are considered as homogeneous unit for the simplicity. MDSM model shown in Figure 1 consists of five regions, each characterized by a complex electric conductivity in time domain:

$\Lambda_i=\sigma_i+\varepsilon_i\partial/\partial t$.

i=np, 1, cp, 2 and e, stands for nucleus plasma, nuclear envelope, cytoplasm, plasma membrane and cell exterior medium (EM), respectively.

In view of exposure of a Jurkat T cell to pulsed electric fields (PEFs) with peak value of E_0, the spatial distribution of the electric potential ϕ in each of five regions satisfies Laplace equations in spherical coordinates (Kotnik and Miklavcic, 2006):

$$\nabla^2\phi_i = 0, (i = np,1,cp,2,e) \quad (1)$$

They have the general forms:

$$\phi_i = (A_i r + B_i / r^2)\cos\theta \quad (2)$$

With r the radii measured from the centre, θ the angle with respect to the direction of applied external field, and A_i, B_i constants specific for each region. Finiteness of the electric potential at r=0 means B_{np}=0 and the spatially uniform field at $r\to\infty$ gives A_e=-E_0.

The remaining eight constants (A_{np}, A_1, B_1, A_{cp}, B_{cp}, A_2, B_2 and B_e) are determined by conditions of continuity of the electrical potential,ϕ and the normal component of electric current density, $\Lambda(n\cdot\nabla\phi)$, at each of the 4 boundaries among 5 regions. n is the normal unit vector of spherical coordinates and Λ is the complex conductivity of a region, $\sigma+\varepsilon s$, in which s is the complex frequency in frequency domain. For example, the pair of continuity

Table 1. Parameters of Jurkat T from references ([a]Hu et al., 2005; [b]Ermolina I et al., 2001).

Parameter	Component	Value
Conductivity (S/m)	PM (σ_2)	[a]5.33×10^{-6}
	CP (σ_{cp})	[a]0.13
	NE(σ_1)	[a]4.33×10^{-3}
	NP(σ_{np})	[a]0.18
	EM(σ_{EM})	[a]0.6
Relative Permittivity	PM(σ_{r2})	[a]7
	CP(σ_{cp})	[a]60
	NE(σ_{r1})	[a]22.8
	NP(σ_{np})	[a]120
	EM(ε_{EM})	[a]80
Geometry Parameters (μm)	Radius cell(R_2)	[b]5.12
	PM thickness(d_2)	[b]0.007
	NP radius(R_1)	[b]4.2
	NE thickness(d_1)	[b]0.04

requirement related to the boundary between the nucleus plasma and nuclear envelope can be described as:

$$A_{np}(R_1 - d_1) = [A_1(R_1 - d_1) + B_1/(R_1 - d_1)^2] \quad (3)$$

$$\Lambda_{np} A_{np} = \Lambda_1[A_1 - 2B_1/(R_1 - d_1)^3] \quad (4)$$

Where $\Lambda_{np}=\sigma_{np}+s\varepsilon_{np}$ and $\Lambda_1=\sigma_1+s\varepsilon_1$

The solutions for eight constants are relatively lengthy, because each of them includes geometric and electric parameters of all five regions from MDSM listed in Table 1. Algebraically, their exact solution is easily obtained when software Maple with inverse Laplace transformation (ILT) is used for the calculation of eight constants.

Laplace equations to layered isotropic sphere are solved with spatially uniform electric field directed along the z-axis. Namely, when r tends to infinity, the electric potential ϕ is:

$$\phi|_{r\to\infty} = -E_0(t) r\cos\theta \quad (5)$$

Finally, the voltages of nuclear plasma, nuclear envelope, cytoplasm, and plasma membrane U_{np}, U_1, U_{cp}, U_2, respectively, can be described as follows:

$$U_{np} = A_{np}(t)(R_1 - d_1)\cos\theta \quad (6)$$

$$U_1 = \{A_1(t)d_1 + B_1(t)[1/R_1^2 - 1/(R_1 - d_1)^2]\}\cos\theta \quad (7)$$

$$U_{cp} = \{A_{cp}(t)(R_2 - d_2 - R_1) + B_{cp}(t)[1/(R_2 - d_2)^2 - 1/R_1^2]\}\cos\theta \quad (8)$$

$$U_2 = \{A_2(t)d_2 + B_2(t)[1/R_2^2 - 1/(R_2 - d_2)^2]\}\cos\theta \quad (9)$$

Electric field with Gaussian shape and monocycle in time domain can be generated by electric pulsed source (Wu et al., 2009). Unfortunately, no analytical expressions can be achieved when cells from MDSM model is exposed to electric field with Gaussian shape and monocycle in time domain. In view of getting a clear physical picture, electric field with Gaussian shape and monocycle in time domain can be described approximately by a sum of ramp functions (Kotnik and Miklavcic, 2006) in time domain. Here, pulsed electric field with Gaussian shape (PEFGS) is written as follows:

$$E = E_0[t/T \cdot H(t) - 2\frac{t-T}{T} \cdot H(t-T) + \frac{t-2T}{T}H(t-2T)] \quad (10)$$

Actually, PEFGS is approximated by a triangular pulse in time domain with Full Width at Half Maximum (FWHM) being T where E_0 is amplitude of PEFGS. Heavside function is:

$$H(t) = \begin{cases} 1 & t \geq 0 \\ 0 & t < 0 \end{cases} \quad (11)$$

PEFGS can be expressed in complex-frequency space with Laplace transformation:

$$E(s) = E_0[\frac{(1-e^{-sT})^2}{s^2 T}] \quad (12)$$

Denoting the complex frequency by s, the differentiation with respect to time is transformed multiplication by *s* with Laplace transformation. The expressions for voltages across nuclear plasma, nuclear envelope, cytoplasm and plasma membrane of Jurkat T cells become functions of s with $\Lambda=\sigma+\varepsilon s$. At the polar of

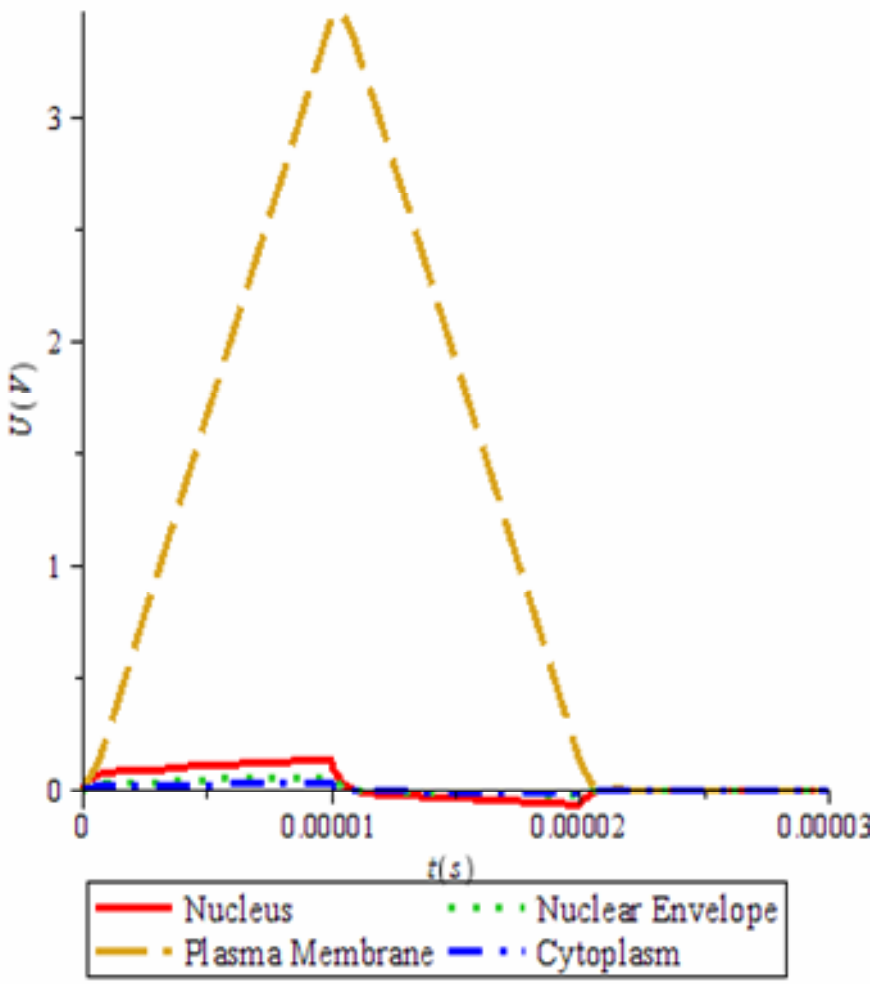

Figure 2. Induced voltages from10μs, 4.8 kV/cm PEF.

Jurkat T cell near anodic electrode (θ=180°) shown in Figure 1, the time courses of the induced voltages across nucleus (in solid line), nuclear envelope (in dot line), cytoplasm (in dash-dot line) and plasma membrane (in dash line), $U_{np}(t)$, $U_1(t)$, $U_{cp}(t)$, and $U_2(t)$ are obtained by inverse Laplace transformation. In our simulations of voltages, four PEFGSs which deposit the same energy density are chosen with time durations being 10 μs, 300, 60 and 10 ns for investigating different responsive voltages of cell parts to those PEFGS. These four PEFs are taken from the Beeb et al. (2003) for explanation of the reported experimental results with MDSM model. Horizontal axis stands for time evolution with unit of seconds(s) and unit of vertical axis is Voltage (V) in Figures 2 and 3.

RESULTS

Response to PEFGS with 10 μs, 4.8 kV/cm

Figure 2 depicts the time courses of the induced voltages across nucleus (solid line), nuclear envelope (dot line), cytoplasm (dash-dot line) and plasma membrane (dash line) $U_{np}(t)$, $U_1(t)$, $U_{cp}(t)$, and $U_2(t)$ with time duration of 10 μs. From Figure 2, plasma membrane of Jurkat T cell plays a dominant role because Jurkat T cell exposed to PEF with 10 μs time duration is shielded by plasma membrane and PEF with 10 μs time duration cannot be accessible to the interior of the cell. In addition, average voltage across the plasma membrane (1.7 V) with time duration being more than 10 μs shown in Figure 2 is greater than the critical voltage (1 V) and critical time duration (2 μs) for irreversible electroporation of plasma membrane (Isambert, 1998). If the breakdown of cell occurs, this electric breakdown was called classical electroporation (Weaver and Chizmadzhev, 1996). In other words, from the analysis in time domain, this electric pulse only targets the plasma membrane.

Response to PEFGS with nanoseconds

In Figure 3(a), for 300 ns, 26 kV/cm pulse, the arranged peak voltages from the highest to the lowest are those

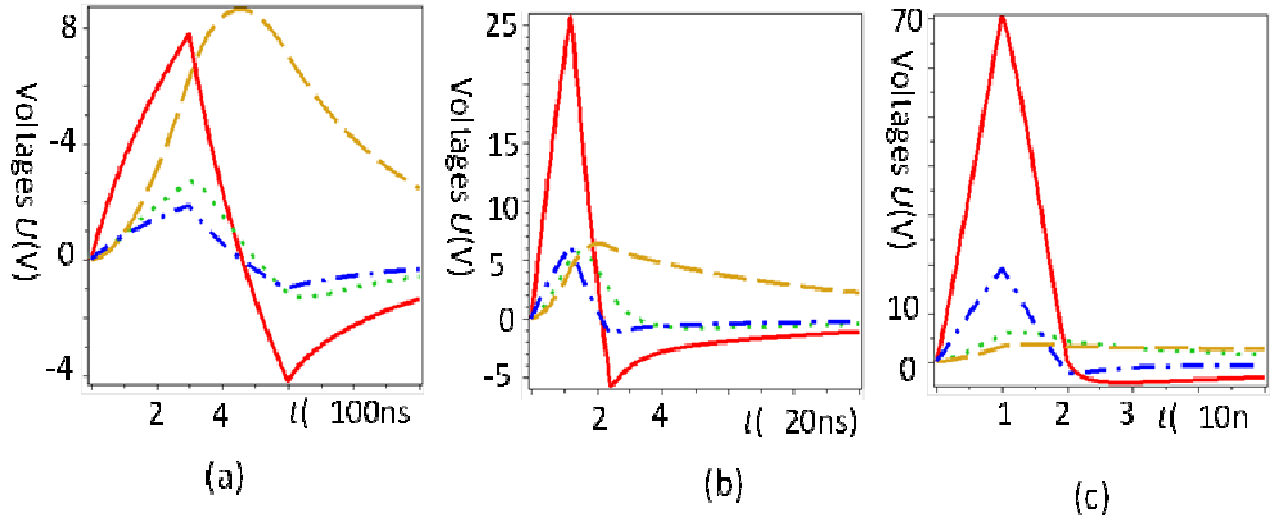

FIGURE 3. Induced voltages *U*(V) *vs.* elapsed time *t* from (a)300ns, 26kV/cm PEF; (b)60ns, 60kV/cm PEF; (c)10ns,150kV/cm PEF. —— nucleus (NP), ––Plasma membrane (PM), –•–cytoplasm(CP),•••Nuclear envelope(NE)

of plasma membrane (dash line), nucleus (solid line), nuclear envelope (dot line) and cytoplasm (dash-dot line). This means PEFs with sub-microsecond time duration gradually penetrate into nuclear plasma and cytoplasm through plasma membrane and nuclear envelope. Note that pulsed voltages across nucleus, nuclear envelope and cytoplasm shown in Figure 3 are asymmetrically bipolar voltage pulses caused by slowing discharging current of plasma membrane (Schoenbach et al., 2001) when the external PEFs fade away.

In Figure 3(b), for 60 ns, 60 kV/cm pulse, the arranged peak voltages from the highest to the lowest are those of nucleus (solid line), cytoplasm (dash-dot line), plasma membrane (dash line), and nuclear envelope (dot line). Note that the peak voltages across the cytoplasm, plasma membrane, nuclear envelope are on the same order of magnitudes, which means all organelles and membranes are targets (Schoenbach et al. 2003).

In Figure 3(c), 150 kV/cm PEF with 10 ns time duration almost completely penetrates through the plasma membrane and nuclear envelope into nuclear plasma and cytoplasm. The voltages of whole-cell are almost completely distributed in nuclear plasma and cytoplasm according to their resistances in series. In this case, the two membranes was almost short out by ultra-fast PEF, so the cytoplasm and nuclear plasma were regarded as connection in series (Schoenbach et al., 2002), and were charged within twenty nano-seconds. If a single PEFGS with nanoseconds range is applied, although voltages across the plasma membrane and across the nuclear envelope are much greater than 1 V in Figures 3a, b and c, plasma membrane and the nuclear envelope are almost intact because the lasting time on membranes is much lower than 2 μs (the critical time duration; Isambert, 1998).

DISCUSSION

Bioelectric effects and time durations of PEF

If bioelectric effects on plasma membrane are determined by the electrical impulse, which is regarded as association with total charge transferred through membranes and described by product of average voltage (U_{PM}) and time duration (t_{PM}) in FWHM from the plasma membrane (Schoenbach et al., 2009), there are some positive correlations between Ethidium homodimer fluorescence (EthD-1 fluorescence) and product of average voltage (AV) and time duration in FWHM of the plasma membrane, which are listed in Table 2. From Table 2, cells exhibited fluorescence increase indicating that the plasma membrane had been breached to allow uptake of EthD-1 when time durations of applied PEFs become longer if three types of pulse train (300 ns, 26 kV/cm; 60 ns, 60 kV/cm; 10 ns, 150 kV/cm) are applied.

Some predictions on nucleus could be made. Products of squared average voltages (U^2_{NP}) and their time duration (t_{NP}) in FWHM across the nuclear plasma go up to maximum when PEFs become shorter, suggesting that the effect of pulse on nuclear plasma tends to severely damaged when PEFs become shorter and shorter in time durations. It is likely that the resistance of nucleus plays a predominate role in comparison to capacitive impedance of nucleus connected in parallel.

As shown in Table 1, the 6th line of Table 3 lists the

Table 2. Fluorescence of Ethidium homodimer (EthD-1),impulse effect on plasma membrane (PM) and cytoplasm.

Type of pulsed electric field (ns, kV/cm)	300, 26	60, 60	10, 150	Control
Average voltage of PM U_{PM} (V)	4.3	3.17	1.83	---
Time duration of voltages across PM t_{PM} (ns)	500	355	135	---
Product of $U_{PM}t_{PM}$ (V.ns) for impulse effect	2150	1125	247	---
EthD-1 fluorescence for classical poration(Beeb et al.,2003)	8.77	5.56	4.30	4.0
Pulsed electric fields on cytoplasm (ns, kV/cm)	230, 25.8	54, 86	10, 260	---

Table 3. Permeability increase in nuclear envelope (NE), dose absorbed by (a) nucleus (Schoenbach et al., 2007) ,(b) the comet tail length (Stacey et al., 2002) and (c) this work.

PEFs (ns, kV/cm)	300, 26	60, 60	10, 150
[a]Dose absorbed by nucleus $U_{NP}^2 t_{NP}$ ($\times 10^3 V^2$.ns)	3.6	9.3	12.7
[c]Average voltage of nuclear envelope (NE) U_1(V)	1.35	2.82	3.00
[c]Time duration of voltages across NE t_1 (ns)	254	80	30
[c]$U_1 t_1$ for impulse effect of NE (V.ns)	342.0	225.6	90.0
[c]DNA damage /permeability increase in nuclear envelope	-/++	+/+	++/-
[b]Increase in tail length of Comet Assay/-Standard Error	22.3%/-3.1%	33.2%/-7.4%	22.9%/-2.8%

electrical impulse of nuclear envelope (NE) which is described in product of average voltage (U_1) and time duration (t_1) in FWHM. As the pulsed become shorter and shorter, the products coming from electrical impulse become smaller and smaller, indicating that permeability in nuclear envelope decreases. If leakage of DNA from nuclear envelope is required for both DNA damage and electro-poration of nuclear envelope by pulse train, in combination of DNA damage and permeability change in nuclear envelope, it suggests from the 6th and 7th line of Table 3 that outflow of more DNA from nucleus to cytoplasm caused by 60 ns, 60 kV/cm could be predicted. Stacey et al. (2002) listed increase in tail length of comet essay (5 pulses), which is listed in the last line of Table 3, and Schoenbach et al. (2007) reported the outflow of DNA by acridine orange (AO) fluorescence from nucleus of HL-60 to entire cytoplasm.

Voltages on cytoplasm induced by three types of PEFs , which are listed in the last line of Table 2, are used as secondary stimuli with the same method described in methodology for Cytochrome C release from mitochondria. Mitochondrial substructure includes outer membrane (OM) with voltage-dependent anion channels (VDAC), inter-membrane Space (IMS), inner membrane (IM) and matrix of Mitochondria (MM) which are depicted in Figure 4.

The parameters on mitochondrial substructure are listed in Table 4 and are given from the study of Gowrishankar et al. (2006). Analysis and calculation are redone as Section 2. Here maximum electric fields (E_{IMS}) and time durations (t_{IMS}) of inter-membrane space (IMS) in FWMH are listed in Table 5 for the detachment of Cytochrome C. Also, average voltages (U_{OM}) and time durations (t_{OM}) of outer membrane/or VDAC are given in Table 5 for Cytochrome C struggling from either outer membrane or VDAC.

From Table 5, 60 ns and 60 kV/cm pulse is the most efficient pulse for Cytochrome C release, which is confirmed by Figure 5 cited from Literature (Schoenbach et al., 2003). Although mitochondrial has a complicated invaginated structure, simple sphere model can easily explain the two steps procedure of cytochrome c release stimulated by electric pulses as follows.

Ott et al. (2002) demonstrated that Cytochrome C released from mitochondria proceeds by a two-step process, first involving the detachment of Cytochrome C from the inner membrane (IM), then permeabilization of the outer membrane (OM). Their data suggest that two distinct pools of Cytochrome C can be mobilized. The first pool is sensitive to electrostatic alternations elicited by changes in ionic strength, surface-charge density or pH, therefore it is likely to reflect Cytochrome C present in the loosely bound conformation. The second pool can be mobilized by oxidative modification of cardiolipin. Neither disrupting the interaction of Cytochrome C with cardiolipin, nor permeabilizing the outer membrane, alone, is sufficient to trigger this protein's release (Ott et al., 2002). This is a biochemical technique to release Cytochrome C from mitochondria to cytosol. We attempt to explain Cytochrome C release with physics method employing two-step process.

Here, the first step can be done by pulsed electric field with appropriate amplitudes and time durations because positively charged Cytochrome C can be exerted enough force for the detachment from cardiolipin as shown in Figure 4. In addition, pulsed electric field shown

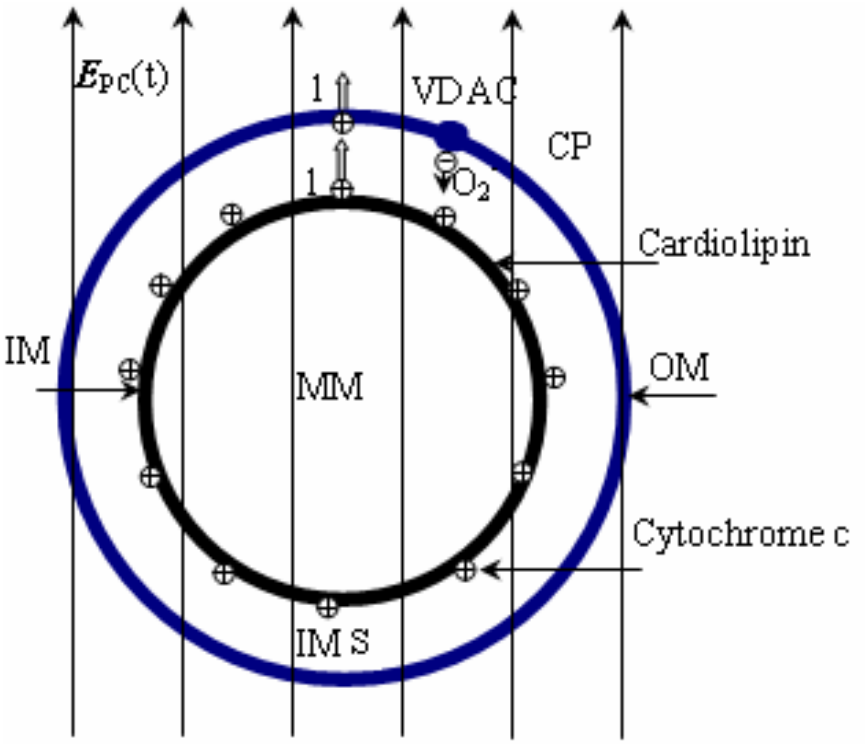

Figure 4. Two-step process of Cytochrome C release (Ott et al.,2002)from mitochondria driven by PEFs.

Table 4. Parameters of mitochondria from Ref (Gowrishankar et al., 2006).

Parameter	Component	Value
Conductivity (S/m)	OM (σ_{OM})	9.5×10^{-7}
	IMS(σ_{IMS})	0.4
	IM(σ_{IM})	47.5×10^{-9}
	MM(σ_{MM})	0.121
	CP (σ_{CP})	0.18
Relative Permittivity	OM(ε_{OM})	12.1
	IMS (ε_{IMS})	54
	IM (ε_{IM})	3.4
	MM (ε_{MM})	54
	CP (ε_{CP})	60
Geometry Parameters (nm)	Radius of Mito. (R_M)	300
	OM thickness (d_{OM})	7
	IMS thickness (d_{IMS})	30

in Figure 4 inhibits the superoxide anion O_2^- exit through Voltage-Dependent Anion Channels (Han et al., 2003), therefore it is likely that increasing peroxidization of cardiolipid or OM is beneficial to detachment of Cytochrome C or permeability increase of OM (Vernier et al., 2009).

From Table 5, 10 ns and 150 kV/cm pulse is bad for Cytochrome C release because the time duration for detachment of Cytochrome C from cardiolipid and accumulation of superoxide anion O_2^- are shortest among

Table 5. Impulse effect on cytoplasm and Cytochrome C release (Beebe et al., 2003).

PEFs on cytoplasm (ns, kV/cm)	230, 25.8	54, 86	10, 260
Electric field of IMS E_{IMS}(kV/cm)	1	9.5	66.8
Time duration of IMS in FWMH t_{IMS} (ns)	200	54	7
Favorable for Cytochrome C detachment/Reason	Not good/weak force	excellent	Bad/shortest time
Average voltage of OM U_{OM}(V)	0.45	0.8	0.89
Time duration of Voltages across OM t_{OM} (ns)	270	100	35
Permeability increase in OM/Reason	Not good/low U_{OM}	excellent	Not Good/shortest time
Cytochrome C release from Jurkat T cancer cell	Middle	Maximum	Little

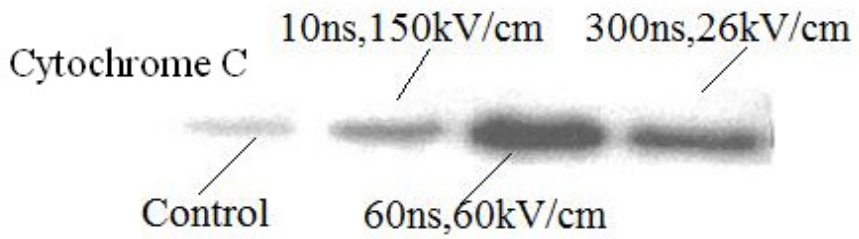

Figure 5. Cytochrome C release induced by three types of nsPEFs (Beebe et al., 2003).

three pulses. In addition, small amounts of released Cytochrome C by 10 ns, 150 kV/cm pulses are attracted by negatively charged cardiolipid for re-binding it, although this kind of pulse train is applied. A single 60 ns and 60 kV/cm pulses could push the positively charged Cytochrome C further than a single 10 ns, 150 kV/cm pulses. If a 60 ns and 60 kV/cm pulse train is applied in comparison to a 10 ns and 150 kV/cm pulse train, Cytochrome C go much further by multiple pulses from cardiolipid and struggle through the outer membrane for release. Compared with a single 60 ns, 60 kV/cm pulse, a single 300 ns, 26 kV/cm pulses exerts much weaker force of Cytochrome C to make Cytochrome C almost intact, but long time peroxidation of cardiolipid by 300ns, 26 kV/cm pulse train is good for dissociation of Cytochrome C from binding locations of cardiolipid. The amounts of free Cytochrome C dissociated from cardiolipid by 300 ns and 26 kV/cm pulse train are between 10 ns, 150 kV/cm pulse train and 60 ns and 60 kV/cm pulse train.

The second step can be optimized by impulse effect on OM from pulses, which are listed in Table 5. From Table 5, for 300 ns, 26 k V/cm pulse train, average voltage of OM (0.45 V), which is lower than the critical voltage (0.5 V) for reversible electroporation of OM is not good for permeability increase of OM, but longer time duration is beneficial to peroxidation of outer membrane for poration of outer membrane. For 10 ns, 150 kV/cm pulse train, fewest amounts of free Cytochrome C and fewest amounts of outer membrane poration led to fewest amounts of Cytochrome C into cytosol. In combination of two-step process for Cytochrome C release, 60 ns, 60 kV/cm PEF is the best pulse among three pulse trains with same pulses (Schoenbach et al., 2003).

Conclusions

Distribution of voltages across nuclear plasma, nuclear envelope, cytoplasm and plasma membrane from Jurkat T cells are analyzed by employing multilayer dielectric sphere model (MDSM) when pulsed electric fields have different time durations with the same energy density. Cytochrome C release can be optimized by analysis of impulse effect on mitochondrial substructures. Our analysis supports the hypothesis that longer, higher intensity pulses affect more targets, including mitochondria and plasma membrane. The analytic results are in good agreements with the reported experimental results and PEF with 60 ns time durations is recommended for apoptosis and necrosis of Jurkat T cells on basis of electric and geometric parameters of Jurkat T cell.

REFERENCES

Beeb SJ, Fox PM, Rec LJ, Stark RH, Schoenbach KH (2002). Nanosecond pulsed electric field (nsPEF) effects on cells and tissues: apoptosis induction and tumor growth inhibition. IEEE Trans. Plasma Sci. 30: 286-292.

Beebe SJ, Fox PM, Rec L, Willis LK, Schoenbach KH (2003). Nanosecond, high-intensity pulsed electric fields induce apoptosis in human cells. FASEB J. 17: 1493-1495.

Ermolina I, Polevaya Y, Feldman Y, Ginburg BZ, Schlesinger M (2001).

Study of normal and malignant white blood cells by time domain dielectric spectroscopy. IEEE Trans on Dielectrics and Electrical Insulation. 8(2): 253-261.
Gowrishankar TR, Esser AT, Vasilkoski Z, Smith KC, Weaver JC (2006). Micro- dosimetry for conventional and supra-electroporation in cells with organelles. Biochem. Biophys. Res. Commun. 341: 1266-1276.
Han D, Antunes F, Canali R, Rettori D, Cadenas E (2003). Voltage-dependent anion channels control the release the super-oxide anion from mitochondria to cytosol. J. Biol. Chem. 278(8): 5557-5563.
Hu Q, Viswanadham S, Joshi RP, Schoenbach KH, Beebe SJ, Blackmore PF (2005). Simulations of transient membrane behavior in cells subjected to a high intensity, ultra-short electric pulse. Phys. Rev. E. 71: 0319141/1-0319141/6.
Isambert H (1998), Understanding the electroporation of cells and artificial bilayer membranes. Phys. Rev. Lett. 80(15): 3404-3407.
Joshi RP, Hu Q, Schoenbach KH (2004). Modeling studies of cell response to ultrashort, high-intensity electric fields-implications for intracellular manipulation. IEEE Trans. Plasma Sci. 32: 1677-1686.
Kennedy SM, Ji Z, Rockweiler NB, Hahn AR, Booske JH, Hagness SC (2009). The role of plasmalemmal-cortical anchoring on the stability of trans-membrane electropores. IEEE Trans. on Dielectrics and Electrical Insulation, 16: 1251-1258.
Kotnik T, Miklavcic D (2006). Theoretical evaluation of voltage inducement on internal membranes of biological cells exposed to electric fields. Biophys J. 90: 480-487.
Ott M, Robertson JD, Gogvadze V, Zhivotovsky B, Orrenius s (2002). Cytochrome C release from mitochondria proceeds by a two-step process. Proc. Natl. Acad. Sci. USA, 99(3): 1259-1263.
Schoenbach KH, Beebe SJ, Buescher ES (2001). Intracellular effect of ultrashort electrical pulses. J. Bioelectromagnetics, 22: 440-448.
Schoenbach KH, Katsuki S, Stark RH, Buescher ES, Beeb SJ (2002). Bioelectrics: new applications for pulsed power technology. IEEE Trans. Plasma Sci. 30: 293-300.
Schoenbach KH, Hargrave B, Joshi RP, Knolb JF, Nuccitelli R, Osgood C, Pakhomov AG , Stacey M, Swanson RJ, White JA, Xiao S, Zhang J, Beeb SJ, Blackmore PF, Buesche ES (2007). Bioelectric effects of intense nanosecond pulses. IEEE Trans. on Dielectrics and Electrical Insulation, 14: 1088-1109.
Schoenbach KH, Joshi RP, Beeb SJ, Baum CE (2009). A scaling law for membrane permeabilization with nanopulses. IEEE Transactions on Dielectrics and Electrical Insulation, 16: 1224-1235.
Smith KC, Neu JC, Krassowska W (2004). Model of creation and evolution of stable electropores for DNA delivery. Biophys. J. 86: 2813-2816.
Stacey M, Stickley J, Fox MP, O'Donnell C, Schoenbach KH (2002). Increased cell killing and DNA damage in cells exposed to ultra-short pulsed electric fields. Annual Report Conference on Electrical Insulation and Dielectric Phenomena.
Vernier PT, Sun Y H, Marcu L, Craft CM, Gundersen MA (2004). Nanosecond pulse electric fields perturb membrane phospholipids in T lymphoblasts. FASEB Lett. 572: 103-108.
Vernier PT, Levine Z A, Wu YH, Joubert V, Ziegler MJ, Mir LM, Tieleman DP (2009). Electroporating fields target oxidatively damaged areas in the cell membrane PLoS ONE, 4(11): 7966/1-7966/8.
Weaver JC, Chizmadzhev YA (1996). Theory of electroporation: a review. Bio-electrochemistry and bioenergetics. 41: 135-160.
Wu MH, Zheng XM, Ruan CL, Yang HC, Sun YQ, Wang S, Zhang KD, Liu H (2009). Photo-resistances of semi-insulating GaAs photoconductive switches illuminated by 1.064 μm laser pulse. J. Appl. Phys. 106: 023101/1-023101/6.
Yao CG, Hu XQ, Mi Y, Li CX, Sun CX (2009). Windows effect of pulsed electric fields on biological cells. IEEE Trans. on Dielectrics and Electrical Insulation. 16: 1259-1266.